Oxygen adsorption on Zr(0 0 0 1) surfaces: Density functional calculations and a multiple-layer adsorption model

ARTICLE *in* SURFACE SCIENCE · JULY 2008

Impact Factor: 1.93 · DOI: 10.1016/j.susc.2008.04.033

6 AUTHORS, INCLUDING:

Shi-Yu Liu
Tianjin Normal University
18 PUBLICATIONS **103** CITATIONS
SEE PROFILE

Yun-Song Zhou
Capital Normal University
96 PUBLICATIONS **699** CITATIONS
SEE PROFILE

Zhenyu Li
University of Science and Technology of Ch…
138 PUBLICATIONS **3,179** CITATIONS
SEE PROFILE

Jinlong Yang
University of Science and Technology of Ch…
510 PUBLICATIONS **11,043** CITATIONS
SEE PROFILE

Surface Science 602 (2008) 2212–2216

Contents lists available at ScienceDirect

Surface Science

journal homepage: www.elsevier.com/locate/susc

Oxygen adsorption on Zr(0001) surfaces: Density functional calculations and a multiple-layer adsorption model

Fu-He Wang [a,*], Shi-Yu Liu [a], Jia-Xiang Shang [b], Yun-Song Zhou [a], Zhenyu Li [c], Jinlong Yang [c]

[a] Department of Physics, Capital Normal University, Xi San Huan Bei Lu 105, Beijing 100037, PR China
[b] School of Materials Science and Engineering, Beijing University of Aeronautics and Astronautics, Beijing 100083, PR China
[c] Hefei National Laboratory for Physical Sciences at Microscale, University of Science and Technology of China, Hefei, Anhui 230026, PR China

ARTICLE INFO

Article history:
Received 30 January 2008
Accepted for publication 26 April 2008
Available online 6 May 2008

Keywords:
Density functional calculations
Adsorption
Surface relaxation and reconstruction
Zirconium

ABSTRACT

The adsorption of oxygen atoms on the Zr(0001) surface is investigated by the use of *ab initio* total energy density functional methods within the generalized gradient approximation. Considering the repulsive interactions between the adsorbed oxygen atoms, a multiple-layer adsorption model (MLAM), in which the adsorbed oxygen atoms take the sites in different adsorption layers, was used. Our calculated results with a $p(2 \times 2)$ unit cell show that the surface face-centered cubic (SFCC) sites are the most favorable sites at the oxygen coverage of 0.25 monolayer (ML). However, the system with one oxygen adatom taking the SFCC sites and the other one taking the octahedral sites between second and third Zr layers (Octa(2,3)) is the most stable configuration at the coverage of 0.50 ML. As the oxygen coverage is increased to 1.0 ML, each of the oxygen atoms prefers taking the SFCC and octahedral sites such as Octa(2,3), Octa(4,5) and Octa(6,7) in the alternate layers, respectively. Our calculated results of the work functions with the MLAM successfully explain the interesting and unusual experimental work function changes upon oxygen adsorption. It should be noticed that the MLAM must be taken into account for oxygen adsorption on the Zr(0001) surface.

1. Introduction

The understanding of the chemisorption of oxygen on metal surfaces is of considerable fundamental interest and important in a number of technological processes such as oxidation, corrosion and heterogeneous catalysis [1]. It is generally believed that the adsorbed oxygen atoms get electrons from metals and become negative ions when they adsorbed on metal surfaces [2–6]. The interactions between the adsorbed oxygen atoms may be attractive such as on Al(111) surface [2], or repulsive such as on transition metal Ru(0001) [3], Rh(111) [4], Pd(111) [5], Ag(111) [6] surfaces.

A representative chemisorption system is oxygen on Zr(0001) surface, which was broadly studied [7–14]. At low temperature, tensor low-energy electron diffraction (TLEED) suggested that an half of oxygen atoms occupy the octahedral sites between the first and the second metal layer and another half take the sites between the second and third layer, when the coverages of oxygen are 0.5 and 1.0 ML [7,8]. The work function decreased about 0.25 eV at the beginning of the oxygen adsorption on the Zr(0001) surface, then increased when the O_2 dose was increased and a subsequent plateau was reached when the O_2 dose is high enough. However, when the adsorbed sample was annealed at the temperature about 560 K, the work function decreased by a further 0.3 eV, and a sharp $p(2 \times 2)$ LEED pattern was formed [12]. The changes of work function and LEED pattern caused by anneal are still not well understood.

Previous first-principles calculations with the local density approximation (LDA) suggested that the most energetic favorable sites for oxygen adsorption on Zr(0001) surface are the octahedral sites between the second and the third layer of Zr(0001) surface, when the coverage of oxygen is more than 0.5 ML [13,14]. However, the surface face-centered cubic (SFCC) sites are the most favorable sites when the calculations were done with the generalized gradient approximation (GGA) [14]. Besides the discrepancies of the prediction for the most energetic favorable sites for oxygen adsorption, the experimental results of changes in the work functions could not be successfully explained by the theoretical calculations. In all the previous calculations, initial geometries were restricted with a layer by layer model. In our recent study on the adsorption of oxygen on Ti(0001) surface, considering the repulsive interactions between the adsorbed oxygen atoms, we have proposed a multiple-layer adsorption model (MLAM) [15]. In this model, oxygen atoms can distribute in different layers, so they can take sites with less repulsive interactions. The experimental

* Corresponding author. Tel.: +86 10 82429161.
E-mail address: wfh-phy@mail.cnu.edu.cn (F.-H. Wang).

0039-6028/$ - see front matter © 2008 Elsevier B.V. All rights reserved.
doi:10.1016/j.susc.2008.04.033

results such as changes in the work functions, LEED patterns, and the ultraviolet photoelectron spectroscopy (UPS) were successfully explained with the MLAM [15].

What is the real structure of the oxygen adsorbed on Zr(0001) surface? Why are there changes in the work functions and LEED patterns? In this paper, we address these questions by first-principles calculations. We find that the most stable configuration is a multiple-layer adsorption. The changes in work function and LEED pattern can be successfully explained by the penetration of oxygen atoms from the surface face-centered cubic (SFCC) sites to the octahedral sites in the alternate subsurface layers, when the sample was annealed.

2. Computational details and models

Using the Vienna *ab initio* simulation package (VASP) [16–18], we performed the density functional theory (DFT) [19,20] calculations within the GGA of the PW91 form [21] for electron exchange and correlation. Here, we employed projector augmented wave (PAW) method [22], as implemented by Kresse and Joubert [23]. We tested *k*-point sampling and kinetic energy cutoff convergence for all supercells. As a result of the convergence tests, we use a kinetic energy cutoff of 400 eV for all calculations. In our calculation, the error of the average binding energy per oxygen atom is less than 0.01 eV. For bulk Zr, a $15 \times 15 \times 15$ Monkhorst–Pack *k*-point mesh [24] for the primitive cell is used. The calculated lattice constant is $a = 3.235$ Å and $c = 5.153$ Å, which agrees very well with experimental result ($a = 3.23$ Å and $c = 5.15$ Å) [25] and previous DFT–GGA result [26].

All the metal surfaces were modeled by a slab of nine metal layers, separated by a vacuum region equivalent to seven bulk metal layers. Oxygen is placed on one side of the slab where the induced dipole moment is taken into account by applying a dipole correction [27,28]. Most calculations for the surfaces were done in $p(2 \times 2)$ surface unit cells with $9 \times 9 \times 1$ Monkhorst–Pack *k*-points [24] in the Brillouin zone. Only in the case for the lower coverage of oxygen $\Theta = 0.25$ ML with the MLAM, a larger $p(4 \times 2)$ cell with $5 \times 9 \times 1$ Monkhorst–Pack *k*-points was used. In our calculations, the bottom three zirconium layers were fixed at their bulk truncated structure, the other atoms were relaxed until the forces on each of them were less than 0.01 eV/Å.

The various oxygen adsorption sites considered in our calculations are shown Fig. 1. We will use the symbol Octa(*i*,*j*) to denote oxygen atoms at the octahedral sites between the *i*th and the *j*th metal layer. Basing on the calculated results in the reference 14 and our calculations, the energies of the systems when oxygen atoms take the tetrahedral sites are relative much higher than those when adatoms take octahedral sites, so we mainly discuss the systems with oxygen atoms taking octahedral sites. There are four metal atoms in each layer in the $p(2 \times 2)$ unit cell. Here, we define the coverage Θ of oxygen as the ratio of the number of adsorbed oxygen atoms to the number of Zr atoms in the first top layer. So there are four oxygen adatoms in the $p(2 \times 2)$ unit cell, when $\Theta = 1.0$ ML. The stability of various O/Zr(0001) systems is analyzed by the calculations of the average binding energy. The average binding energy per oxygen atom is defined as

$$E_b = \frac{1}{N_O^{atom}}[E_{O/Zr(0001)}^{slab} - (E_{Zr(0001)}^{slab} + N_O^{atom} E_O^{atom})],$$

where N_O^{atom} is the number of oxygen atoms in the unit cell, $E_{O/Zr(0001)}^{slab}$, $E_{Zr(0001)}^{slab}$ and E_O^{atom} represent the total energies per unit cell of the oxygen adsorbed Zr slab, the clean Zr slab, and a free oxygen atom, respectively.

3. Results and discussion

3.1. The relative stability of oxygen adsorption sites

In order to compare with the previous DFT results [13,14] we have calculated the adsorption of oxygen on Zr(0001) surface with the single-layer adsorption model (SLAM), in which the oxygen adatoms are restricted in the same adsorption layer. Only a part of the calculated binding energies for the systems with relative lower energies are plotted in Fig. 2. In the SLAM, the most stable sites for oxygen atoms are the SFCC sites. This result is in agreement with the GGA-based result of Jomard et al. [14]. The binding energies for oxygen atoms to occupy the tetrahedral sites are much higher than those for oxygen atoms to occupy the octahedral sites. For example, the binding energies for oxygen atoms to occupy the tetrahedral site between second and third layer is −7.71 eV, but it is −8.9 eV for oxygen to take Octa(2,3) site, when the oxygen coverage is 0.25 ML. This result is also in agreement with the DFT result of Jomard et al. [14].

An important point should be noticed. The average binding energy per oxygen atom is increased when the coverage of oxygen is increased. This reflects the repulsive interactions between adsor-

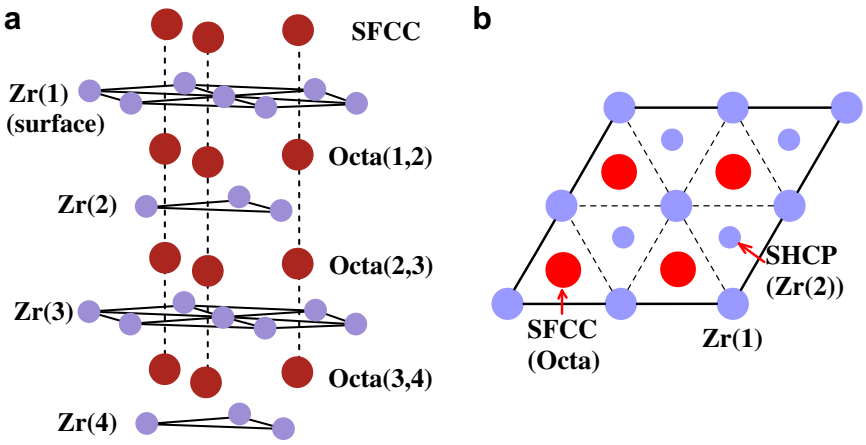

Fig. 1. (a) The three-dimensional structure model of the possible adsorption octahedral sites for oxygen atoms to take at the Zr(0001) surface, and (b) the top view of the $p(2 \times 2)$ unit cell. Large black circles represent the possible adsorption octahedral sites for oxygen atoms. In (b), the large and small grey circles represent Zr atoms in the first and second top layers; the surface hexagonal close-packed (SHCP) sites are directly over the Zr atoms in the second top layer. Here, Octa(*i*,*j*) means the octahedral site between the *i*th and the *j*th metal layer.

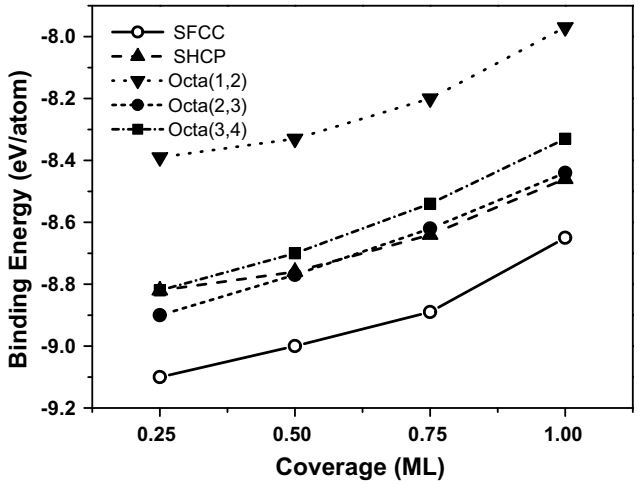

Fig. 2. The calculated binding energies for oxygen atoms to take different adsorption sites with the SLAM at different oxygen coverage.

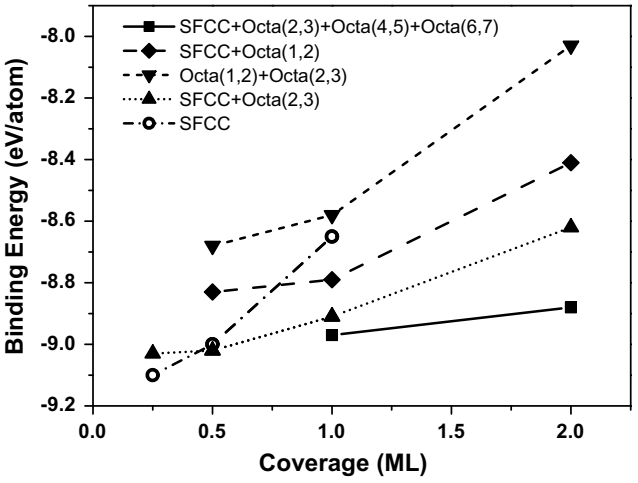

Fig. 3. Some typical calculated binding energies for oxygen atoms to take different adsorption sites with both SLAM and MLAM at different oxygen coverage. The energies for oxygen coverage $\Theta = 0.25$ ML are calculated in the $p(4 \times 2)$ cell. The same number of oxygen atoms distribute in each layer, when they take the combination sites such as SFCC + Octa(1,2) and Octa(1,2) + Octa(2,3), etc.

bates with the decrease of O–O distance. Such a behavior has been also found when oxygen adsorbed on transition metals such as Ru, Rh, Pd, Ag [29]. To discuss the possibility of bulk dissolved oxygen, we also calculate the binding energy of one oxygen atom in an octahedral interstitial site in a large $(4 \times 4 \times 2)$ Zr bulk unit cell with 64 metal atoms, where all the atomic positions are allowed to relax. The calculated binding energy of bulk dissolved oxygen is −8.77 eV. It can be clearly seen that the bulk dissolved oxygen is more favorable than the surface adsorption when $\Theta \geqslant 1.00$ ML.

From the calculated results with the SLAM, it was found that there are repulsive interactions between two adsorbed oxygen atoms when they take the sites with shorter distances, and the bulk dissolved oxygen is more favorable than the surface adsorption when $\Theta \geqslant 1.00$ ML. This make us to use the MLAM to study the structure of oxygen adsorbed Zr(0001) surface. In the MLAM, the oxygen adatoms can be distributed into different layers and take the sites with distance as long as possible. Several possible adsorption structures with the MLAM are studied. In each structure, O atoms can occupy several types of sites. For example, SFCC + Octa(1,2) means O atoms can occupy SFCC and Octa(1,2) sites. For each structure, the most stable configuration is found. The average binding energies for them are listed in Table 1. In order to see clearly, some typical results are plotted in Fig. 3. Several points should be noted. First, at the lower coverage of oxygen, the SFCC sites are the most stable position for oxygen atoms to take, however, they are not the most stable sites for oxygen atoms to occupy, when the coverage $\Theta \geqslant 0.50$ ML. So the oxygen atoms will penetrate into the subsurface when the oxygen coverage is equal to or higher than 0.50 ML and the temperature is high enough. Second, it is impossible for oxygen atoms to take the combination sites of the SHCP with octahedral sites, because the energies of the systems with oxygen atoms taking combination sites of the SHCP with octahedral sites are higher than those of the systems with oxygen atoms taking combination sites of the SFCC with octahedral sites. For example, the binding energies are −8.84 eV and −9.02 eV for the systems with SHCP + Octa(2,3) and SFCC + Octa(2,3), respectively. Third, it is impossible for oxygen atoms to take the sites in the adjacent layers such as the combination of SFCC + Octa(1,2) and Octa(1,2) + Octa(2,3). This result does not support the TLEED analysis results [7–9]. From many possible surface structure models, Wang et al. used the TLEED method [30,31] to optimize the reliability factor R_P and concluded that an half of the oxygen atoms occupy the octahedral sites between the first and second metal layers, i.e., Octa(1,2), another half take those between the second and third metal layers, i.e., Octa(2,3), when the oxygen coverage is 0.5 [7], and 1.0 ML [8] an half take the SFCC sites and another half take the tetrahedral sites between the first and second metal layers when the coverage is 2.0 ML[9]. Unfortunately, Wang et al. only considered the sites in adjacent layers such as SFCC + Octa(1,2), Octa(1,2) + Octa(2,3), etc., when they designed the initial possible structures. It can be clearly seen from our calculated results that the most stable system with the same coverage of oxygen is that with oxygen atoms taking the combination sites such as SFCC, Octa(2,3), Octa(2,3) and Octa(4,5), etc. in alternate layers, when the coverage of oxygen is higher than or equal to 0.5 ML. It is expected that the optimized reliability factor R_P should be smaller for the structures with each of the adsorbed oxygen atoms taking the SFCC, Octa(2,3) and Octa(4,5) etc. sites. In these cases, only one oxygen atom in each adsorption layer within the $p(2 \times 2)$ unit cell. It just correspond to the coverage of 0.25 ML for each adsorption layer, though the total oxygen coverage is 0.5 ML or 1.0 ML, etc. Our definition of oxygen coverage is the ratio of the total number of adsorbed oxygen atoms to the number of Zr atoms in the first top layer. As a result, the oxygen adsorbed Zr(0001) surface with $\Theta \geqslant 0.5$ ML should change into $p(2 \times 2)$ structure, when it is heated in proper temperature. This is in good agreement with experimental results [7–11].

From our calculated results of the binding energies of oxygen with the MLAM, oxygen atoms show a tendency to incorporate into the zirconium bulk, as the increase of the oxygen coverage.

Table 1
The average binding energy E_b (eV) per O atom in the most stable configurations in each sites combination structures with the MLAM for the oxygen coverage $0.50 \leqslant \Theta \leqslant 2.00$ ML

Adsorption site	0.50 (ML)	1.00 (ML)	2.00 (ML)
SFCC	−9.00	−8.65	–
SFCC + Octa(1,2)	−8.83	−8.79	−8.41
Octa(1,2) + Octa(2,3)	−8.68	−8.58	−8.03
SFCC + Octa(2,3)	−9.02	−8.91	−8.62
Octa(2,3) + Octa(3,4)	−8.86	−8.74	−8.28
Octa(2,3) + Octa(4,5)	−9.02	−8.80	−8.52
SFCC + Octa(2,3) + Octa(4,5) + Octa(6,7)	–	−8.97	−8.88

For comparison, those of the most stable structures (SFCC) with the SLAM are also listed.

However, the energies of the systems with oxygen atoms taking the SFCC and the octahedral sites within the surface region are still lower than that of the oxygen dissolved bulk. Therefore, in practice, there should be an activation barrier between interlayer ordering within the whole surface region and bulk randomization.

3.2. Interlayer spacings relaxation

For each system studied above, we compute the variations of the interlayer distances with respect to the bulk Zr value. There are corrugations of the Zr layers when the octahedral sites are partially occupied. So, the interlayer spacing d_{ij} is calculated using the average values for the z-coordinate of the Zr planes. As did in references 13 and 14, we define a ratio of the change of interlayer spacings Δ_{ij} as follows:

$$\Delta_{ij} = (d_{ij} - d_0)/d_0,$$

where d_{ij} is the distance between the ith and jth Zr planes and d_0 the interlayer distance in bulk Zr. Some typical results are listed in Table 2.

From Table 2, it can be found that most of the changes occur in the top three layers. Compared to the bulk value, the interlayer spacing between the first and second top layers of the clean surface is contracted, and that between the second and third top layers is expanded, which is consistent with previous theoretical results [13,26].

For the oxygen covered surface, our calculated results with the SLAM show that Δ_{12} increases from −6.1% to 4.7% as the coverage of the oxygen is increased from 0.0 to 1.0 ML. The reason may be that the electrons are transferred from zirconium atoms to the oxygen atoms and the electron density between zirconium atoms in the first and second top layer is decreased, and the metallic bonds between the first and second top layer zirconium atoms are thus weakened. In the case of Θ = 1.0 ML, our calculated results with the MLAM show that the interlayer spacings between the layers which sandwich the oxygen layer are expanded, and the Zr atoms near the oxygen atoms are pushed away, as a result, Δ_{34} and Δ_{56} are decreased. Comparing the calculated results with the MLAM to those with the SLAM, the changes of the relaxations induced by oxygen atoms with the MLAM are much smaller than those with the SLAM. For example, in the case of Θ = 1.0 ML, compared to the clean surface, the maximum of the changes of Δ_{ij} with the MLAM is 3.2% (the change of Δ_{45} from −0.2% to 3.0%), while it is 10.8% (the change of Δ_{12} from −6.1% to 4.7%) with the SLAM. This may be one of the origin that the combination sites such as SFCC + Octa(2,3) + ⋯⋯ are more favorable than the sites only in the same layer such as SFCC or Octa(2,3), etc.

Table 2
Interlayer relaxations (in %) calculated with the SLAM and MLAM

	Δ_{12}	Δ_{23}	Δ_{34}	Δ_{45}	Δ_{56}	Δ_{67}
Clean surface						
Present cal. GGA	−6.1	2.2	0.4	−0.2	−0.2	0.5
GGA[a]	−6.1	2.3	0.7	−0.5	0.5	–
LDA[b]	−4.7	1.2	1.0	−0.6	0.3	–
Θ = 0.25 ML						
SFCC	−3.4	1.8	0.0	0.1	−0.5	0.7
Θ = 0.50 ML						
SFCC	−0.9	1.4	−0.4	0.4	−0.6	0.7
SFCC + Octa(2,3)	−3.0	3.6	−0.4	0.3	−0.6	0.5
Θ = 1.0 ML						
SFCC	4.7	0.6	−0.8	1.3	−0.7	1.1
SFCC + Octa(2,3) + Octa(4,5) + Octa(6,7)	−3.0	3.7	−0.9	3.0	−1.3	2.8

[a] Ref. [26].
[b] Ref. [13].

3.3. Changes in work functions

In order to explain experimental results of changes in work functions, we have calculated the work functions for the clean and the oxygen adsorbed Zr(0001) surfaces with both SLAM and MLAM. Our calculated work function for the clean surface is 4.24 eV, which agree well with experimental value 4.33 eV [32], and 4.05 eV [33], and previous DFT result 4.26 eV [13]. In comparison to the clean Zr(0001) surface, the changes in work functions $\Delta\phi$ for the different adsorbed systems are shown in Fig. 4 for the range of oxygen coverage $0 \leqslant \Theta \leqslant 1$ ML with both SLAM and MLAM.

At low temperature (82 K), the work function decreased about 0.25 eV at the beginning of the oxygen adsorption on the Zr(0001) surface, then increased when the O_2 dose was increased and a subsequent plateau was reached when the O_2 dose is high enough [12]. It is clearly seen that the changes in the work functions of the most stable systems with the SLAM is in excellent agreement with the low temperature experimental results, where oxygen atoms only occupy the SFCC sites. When the adsorbed sample was annealed at the temperature about 560 K, the work function decreased by a further 0.3 eV, and a sharp p(2 × 2) LEED pattern was formed [12]. Similar results were obtained when the Zr(0001) surface was oxidized at room temperature and annealed at temperature of 473 K [11]. Now, using MLAM, we can explain these experimental puzzle. When the oxygen adsorbed sample was annealed at higher temperature, the adatoms on the surface would overcome the barrier and penetrate into the subsurface. Of course, they would occupy the most stable sites. From Fig. 4, it can be found that the work functions of the most stable systems are almost constant when the oxygen coverage is more than 0.25 ML. Compared to those SLAM systems, the work functions decreased a lot. It should be noted that all the structures of the most stable systems are $p(2 \times 2)$, because there is only one oxygen atom in each of adsorbed layers.

Another point should be stressed. It is general believed that the work functions increase (decrease) when the negatively charged adatom such as oxygen adsorb above (below) the surface [34]. Intuitively, we expect that the charge is transferred from the metal atoms to the more electronegative oxygen atoms. When the oxygen coverage is higher than 0.50 ML, the general expression is

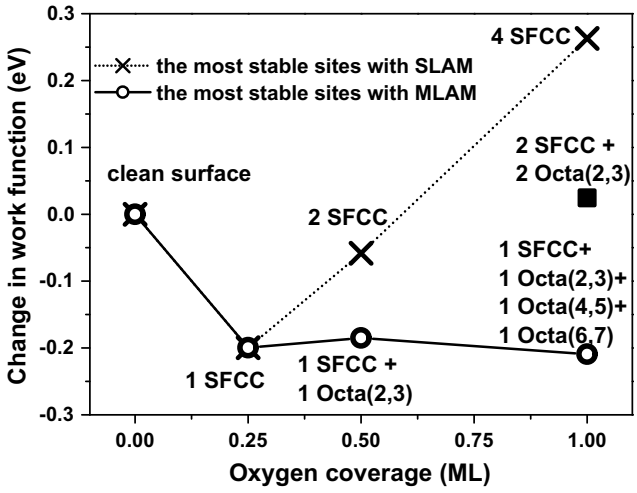

Fig. 4. The calculated changes in work functions of the systems with oxygen atoms taking different sites as a function of oxygen coverage. As a guideline, the trends of work functions of the most stable systems with SLAM and MLAM are plotted with dot and solid line, respectively.

correct. However, the work function of the system with 0.25 ML of oxygen taking the SFCC sites decreases in comparison to the clean surface. The similar behavior has also been found in the O/Ti(0001) [15], and O/Al(111) [2] systems. As pointed by Leung et al, the work function changes are not only decided by the quantity and the sign of the charge transferred, but also by the details of the charge redistribution [35]. It can not be decided only from the relative changes of the work functions that the oxygen atoms reside on surface or in subsurface.

4. Conclusion

In summary, considering the repulsive interactions between the adsorbed oxygen atoms on Zr(0001) surface, we need use the MLAM, in which the oxygen adatoms can be distributed into different layers and take the sites with distance as long as possible. The first-principle calculations with this model show that the SFCC sites are the most favorable sites at the coverage of 0.25 ML; however, the system with one oxygen adatom taking the SFCC sites and each of the others taking the octahedral sites in alternate subsurface layers is the most stable configuration when the coverage of oxygen is equal to or higher than 0.5 ML. The experimental results of work function changes after anneal are successfully elucidated with MLAM. We anticipate that the MLAM may also be generally valid for other gas atom adsorption on some other metal surfaces, and it should be considered in future theoretical modeling.

Acknowledgements

This work is partially supported by the Foundation for National Excellent Doctoral Dissertations of China (No. 200334), and by the National Natural Science Foundation of China (No. 20533030).

References

[1] C. Stampfl, M.V. Ganduglia-Pirovano, K. Reuter, M. Scheffler, Surf. Sci. 500 (2002) 368.
[2] A. Kiejna, B.I. Lundqvist, Phys. Rev. B 63 (2001) 085405.
[3] C. Stampfl, M. Scheffler, Phys. Rev. B 54 (1996) 2868.
[4] M.V. Ganduglia-Pirovano, M. Scheffler, Phys. Rev. B 59 (1999) 15533.
[5] M. Todorova, K. Reuter, M. Scheffler, J. Phys. Chem. B 108 (2004) 14477.
[6] W.X. Li, C. Stampfl, M. Scheffler, Phys. Rev. B 65 (2002) 075407.
[7] Y.M. Wang, Y.S. Li, K.A.R. Mitchell, Surf. Sci. 342 (1995) 272.
[8] Y.M. Wang, Y.S. Li, K.A.R. Mitchell, Surf. Sci. Lett. 343 (1995) 1167.
[9] Y.M. Wang, Y.S. Li, K.A.R. Mitchell, Surf. Sci. 380 (1997) 540.
[10] K.C. Hui, R.H. Milne, K.A.R. Mitchell, W.T. Moore, M.Y. Zhou, Solid State Commun. 56 (1985) 83.
[11] C.-S. Zhang, B.J. Flinn, I.V. Mitchell, P.R. Norton, Surf. Sci. 245 (1991) 373.
[12] K. Griffiths, J. Vac. Sci. Technol. A 6 (1988) 210.
[13] M. Yamamoto, C.T. Chan, K.M. Ho, S. Naito, Phys. Rev. B 54 (1996) 14111.
[14] G. Jomard, A. Pasturel, Appl. Surf. Sci. 177 (2001) 230.
[15] S.-Y. Liu, F.-H. Wang, Y.-S. Zhou, J.-X. Shang, J. Phys.: Condens. Matter 19 (2007) 226004.
[16] G. Kresse, J. Hafner, Phys. Rev. B 48 (1993) 13115.
[17] G. Kresse, J. Furthmüller, Phys. Rev B. 54 (1996) 11169.
[18] G. Kresse, J. Furthmüller, Comput. Mater. Sci. 6 (1996) 15.
[19] P. Hohenberg, W. Kohn, Phys. Rev. 136B (1964) 864.
[20] W. Kohn, L.J. Sham, Phys. Rev. 140A (1965) 1133.
[21] J.P. Perdew, J.A. Chevary, S.H. Vosko, K.A. Jackson, M.R. Pederson, D.J. Singh, C. Fiolhais, Phys. Rev. B 46 (1992) 6671.
[22] P.E. Blöchl, Phys. Rev. B 50 (1994) 17953.
[23] G. Kresse, D. Joubert, Phys. Rev. B 59 (1999) 1758.
[24] H.J. Monkhorst, J.D. Pack, Phys. Rev. B 13 (1976) 5188.
[25] C. Kittel, Introduction to Solid State Physics, seventh ed., John Wiley & Sons Inc., New York, 1996.
[26] G. Jomard, T. Petit, L. Magaud, A. Pasturel, Phys. Rev. B 60 (1999) 15624.
[27] J. Neugebauer, M. Scheffler, Phys. Rev. B 46 (1992) 16067.
[28] L. Bengtsson, Phys. Rev. B 59 (1999) 12301.
[29] M. Todorova, W.X. Li, M.V. Ganduglia-Pirovano, C. Stampfl, K. Reuter, M. Scheffler, Phys. Rev. Lett. 89 (2002) 096103.
[30] P.J. Rous, Prog. Surf. Sci. B 39 (1992) 3.
[31] P.J. Rous, M.A. Van Hove, G.A. Somorjai, Surf. Sci. B 226 (1992) 15.
[32] H. Malamud, A. Krumbein, J. Appl. Phys. 25 (1954) 591.
[33] D.E. Eastman, Phys. Rev. B 2 (1970) 1.
[34] J. Hölzl, F.K. Schulte, Solid State Physics, Springer, Berlin, 1979. p. 1.
[35] T.C. Leung, C.L. Kao, W.S. Su, Y.J. Feng, C.T. Chan, Phys. Rev. B 68 (2003) 195408.